

# ON-LINE DETECTION/ESTIMATION SCHEME IN LASER DOPPLER ANEMOMETRY

FRÉDÉRIC GALTIER AND OLIVIER BESSON

ENSICA, Department of Avionics and Systems, 1 Place Émile Blouin, 31056 Toulouse, France.

Email: galtier,besson@ensica.fr

## ABSTRACT

Laser anemometers have become a promising technique for estimating velocities in a flow. In this paper, we study their use for on-board aircraft speed of flight estimation. More specifically, this paper addresses the problem of simultaneous detection of the arrival of aerosol particles in a laser anemometer and estimation of their velocity. A joint detection-estimation scheme is proposed. A Likelihood Ratio Test is presented and considerations about the specificities of the problem are used to calculate the threshold. Computationally efficient algorithms for estimating the parameters of interest are derived and on-line implementation issues are addressed. Numerical examples attest for the performance of the method, on both simulated and real data recorded during a flight test.

## 1. PROBLEM FORMULATION

We consider the problem of estimating aircraft's speed from an on-board laser anemometer. This system is based on two coherent laser beams which are crossed and focused in the vicinity of the aircraft. Hence, a symmetric interference fringe pattern composed of bright and dark fringes is generated. When a particle of aerosol, with speed  $V$ , crosses the successive dark and bright fringes, it will scatter and not scatter light according to its velocity. It can be shown the signal recorded by a photodetector consists of a sinusoidal signal (whose frequency is representative of particle's velocity, hence of aircraft's speed) with a Gaussian shaped time-varying amplitude. In previous papers [1, 2], we addressed the problem of estimating the frequency of such a signal. Here, we are concerned with the detection of arrival of an aerosol. As a matter of fact, since the flow is not continuous, particle appears randomly on the sides of the fringes pattern and then crosses the probe volume. A key point, prior to or in conjunction with estimation, is to detect whether a particle is currently present. Since we are looking for on-line detection, the problem can be adequately formulated as deciding, from a sliding window of  $N = 2T + 1$  data points, between the two following hypotheses:

$$\mathbf{H}_0 : x(t) = b(t) \text{ or } \mathbf{H}_1 : x(t) = s(t - t_c) + b(t)$$

where the parameter  $t_c \in ]-2T, 2T[$  is representative of the fact that a particle has begun to appear in the probe volume and contributes to the recorded signal. The case  $t_c = 0$  corresponds to a particle at the center of the probe volume.  $b(t)$  is assumed to be a

sequence of independent and identically Gaussian distributed random variables  $\sim N(0, \sigma_b^2)$ .  $s(t)$  denotes the useful signal and is given by the following theoretical expression

$$s(t) = A \exp \{ -2\alpha^2 f_d^2 t^2 + j\omega_d t \} \quad (1)$$

where  $A$  denotes the amplitude of the signal,  $\omega_d \triangleq 2\pi f_d$  is related to the particle's velocity and  $\alpha$  is an optical parameter of the system. Thus, the interesting information is the flow velocity  $V$  directly related to the frequency parameter  $f_d$  of  $s(t)$  in (1). Once  $\mathbf{H}_1$  is assumed, an estimate of the Doppler frequency  $f_d$  should be made available. However, [1] showed that the Cramér-Rao Bound on the estimated signal's parameter  $f_d$  is minimum for  $t_c = 0$ . Since the CRB does not significantly vary around  $t_c = 0$ , a frequency estimate will be considered as valid when both  $\mathbf{H}_1$  is true and  $t_c = 0$  is small, classically  $-10 \leq t_c \leq 10$ .

In the sequel, we briefly present an on-line joint detection/estimation scheme based on Neyman-Pearson test. The reader is referred to [3] for detailed derivations that could be skipped here.

## 2. LIKELIHOOD RATIO TEST

We begin with a Likelihood Ratio Test to tackle the detection problem. From the assumption made on  $b(t) \sim N(0, \sigma_b^2)$ , one could prove that the likelihood ratio test can be written in the form [3, 4, 5]

$$\Lambda(\mathbf{x}) = \frac{p(\mathbf{x} | \mathbf{H}_1)}{p(\mathbf{x} | \mathbf{H}_0)} = \frac{\exp \left\{ -\frac{\|\mathbf{x} - A \cdot \mathbf{s}_c\|^2}{\sigma_b^2} \right\}}{\exp \left\{ -\frac{\|\mathbf{x}\|^2}{\sigma_b^2} \right\}} \underset{\mathbf{H}_0}{\overset{\mathbf{H}_1}{\gtrless}} \eta \quad (2)$$

$$\text{or } l(\mathbf{x}) = \ln(\Lambda(\mathbf{x})) = \frac{\|\mathbf{x}\|^2 - \|\mathbf{x} - A \cdot \mathbf{s}_c\|^2}{\sigma_b^2} \underset{\mathbf{H}_0}{\overset{\mathbf{H}_1}{\gtrless}} \gamma \quad (3)$$

These forms suggest that we resort to a Neyman-Pearson test [4, 5] using the probability of false alarm  $P_{FA}$  and probability of detection  $P_D$  to fix the threshold  $\eta$  of the test. From (2) and (3), it directly ensues that

$$P_{FA} = \int_{\eta}^{+\infty} p(\Lambda | \mathbf{H}_0) d\Lambda = \int_{\gamma}^{+\infty} p(l | \mathbf{H}_0) dl \quad (4)$$

$$P_D = \int_{\eta}^{+\infty} p(\Lambda | \mathbf{H}_1) d\Lambda = \int_{\gamma}^{+\infty} p(l | \mathbf{H}_1) dl \quad (5)$$

In these equations  $p(\Lambda | \mathbf{H}_i)$  ( $p(l | \mathbf{H}_i)$ ) denotes the probability density function of the (log-)likelihood ratio  $\Lambda(\mathbf{x})$  ( $l(\mathbf{x})$ ) when  $\mathbf{H}_i$  is true. With the expression (3) and the assumption made on  $b(t)$ , it

comes

$$l(\mathbf{x}) \sim N\left(-\frac{|A|^2 \|s_c\|^2}{\sigma_b^2}, 2\frac{|A|^2 \|s_c\|^2}{\sigma_b^2}\right) \text{ under } \mathbf{H}_0$$

$$l(\mathbf{x}) \sim N\left(\frac{|A|^2 \|s_c\|^2}{\sigma_b^2}, 2\frac{|A|^2 \|s_c\|^2}{\sigma_b^2}\right) \text{ under } \mathbf{H}_1 \quad (6)$$

Therefore, with  $SNR \triangleq \frac{A^2}{\sigma_b^2}$ , (4) and (5) become

$$P_{FA} = 1 - \text{erf}\left(\frac{\gamma + SNR \cdot \|s_c\|^2}{\sqrt{2SNR} \cdot \|s_c\|}\right) \quad (7)$$

$$P_D = 1 - \text{erf}\left(\frac{\gamma - SNR \cdot \|s_c\|^2}{\sqrt{2SNR} \cdot \|s_c\|}\right) \quad (8)$$

erf is the classical abbreviation for the *error function*. These last expressions allow to plot the receiver operating characteristics (ROC) and then to choose the correct  $\gamma$ . We do not normalize the mean and variance of  $l(\mathbf{x})$  in (6) by including  $\sigma_b^2$  and  $\|As_c\|^2$  in the threshold  $\gamma$  in order to keep a  $\gamma$  adapted to all configurations of the received signal. By looking at the ROC for various  $SNR$  and  $t_c$  versus  $\gamma$ , we noticed that all the corresponding  $P_{FA}$  curves are super-imposed, indicating a very high slope around  $\gamma = 0$ . The best compromise would be to choose  $\gamma = 0$ : this value of  $\gamma$  ensures a  $P_{FA}$  minimum and a  $P_D$  maximum over all possible scenarios for the laser signal. However, this is not fully satisfactory for the application considered here. It should also be noticed that  $P_D \simeq 1$  for all  $t_c \in [-T, T]$ . Taking  $\gamma > 0$  involves a very low  $P_{FA}$  but decreases the corresponding  $P_D$ . In the same way  $\gamma < 0$  ensures a  $P_D \rightarrow 1$  but at the expense of increasing  $P_{FA}$ . In fact, it is necessary to **ensure a very low probability of false alarm**  $P_{FA}$ : we do not want to make any estimation if the signal only consists of noise. In contrast, it is **less critical to ensure a high  $P_D$  unless  $t_c$  is close to zero**. In order to select the value of  $\gamma$  to be retained, we adopt the **following rule**:  $\gamma$  is chosen such that  $\gamma > 0$  and  $P_D \geq 0.995$  at least for  $-\frac{T}{2} \leq t_c \leq \frac{T}{2}$ . This condition should hold over all possible values of  $f_d$  and  $SNR$ . Experimental results indicate that the signals delivered by the laser anemometer exhibit frequencies  $0.02 \leq f_d \leq 0.20$  and  $0 \leq SNR \leq 20\text{dB}$ . Figure 1 represents the maximum value of  $\gamma$  satisfying this condition versus  $SNR$  for various frequencies  $f_d$ . It appears that  $\gamma = 7.5$  is the theoretical value of the threshold which will ensure the conditions. Note that choosing  $0 < \gamma < 7.5$  will imply  $P_D > 0.995$  for all frequencies and  $SNR$ 's but at the expense of increasing  $P_{FA}$ .

### 3. ON-LINE ESTIMATION AND DETECTION.

Let us consider that a set  $\mathbf{x}$  of  $N$  samples has been delivered by the anemometer. Before testing the possibility for this set to be under  $\mathbf{H}_0$  or  $\mathbf{H}_1$ , the first task is to estimate the parameter vector  $\hat{\theta} = \{\hat{A}, \hat{f}_d, \hat{t}_c, \hat{\sigma}_b^2\}$ . The estimation procedure is mainly faced with two major constraints:

- 1° Estimation of  $\hat{\theta}$  should be a computationally efficient task easily amenable to on-line implementation.
- 2° The estimator should give plausible values of  $\hat{\theta}$  under both  $\mathbf{H}_0$  and  $\mathbf{H}_1$ , i.e. robust to modelling errors.

A Maximum Likelihood Estimator (MLE) of the vector  $\theta$  was derived in [1]. In the case under study now, this particular estimator

may involve several problems which can be avoided using others methods. [2] proposed the frequency phase based estimator:  $\hat{\omega}_d = \arg \min_{\omega} \sum_{m=1}^M [\angle \hat{r}_x(m) - m\omega]^2$ , which leads to

$$\hat{\omega}_d = \frac{6}{M(M+1)(2M+1)} \sum_{m=1}^M m \angle \hat{r}_x(m) \quad (9)$$

$$\text{where } \hat{r}_x(m) = \sum_{k=-T}^{T-m} x^*(k) \cdot x(k+m) \quad (10)$$

is an unbiased estimator of the covariance function of  $\mathbf{x}$ .  $M$  is an user defined parameter whose optimal choice is  $M \simeq \frac{T}{3}$  (see [2]). We now examine the respective merits of these two estimators with regards to the constraints mentioned above.

- The joint ML estimation of  $f_d$  and  $t_c$  is a computationally burdensome problem. Moreover, it is not possible to use this method on-line. In contrast, estimation of the correlation sequence is computationally simple and easy to implement on-line. Indeed, when a new signal's sample  $x(T+1)$  is available, we readily have:  $\hat{r}_{x|T}(m) = \hat{r}_{x|T}(m) + x^*(T+1-m) \cdot x(T+1) - x^*(-T) \cdot x(-T+m)$  for  $m = 1, \dots, M$ .  $\hat{r}_{x|T}(m)$  denote the correlation lags (10) of the set  $\{x(t)\}_{t=-T, \dots, T}$ .

- However, the phase-based estimator does not provide an estimate of  $t_c$ . From (1), under  $\mathbf{H}_1$  and in the noise free case we obviously have:  $t_c = \arg \max_t |x(t)|$ . We propose to use this sub-optimal estimator in the noisy case

$$\hat{t}_c = \arg \max_t |x(t)| \quad (11)$$

This ensures a very fast computational method. For high  $SNR$ 's it directly comes  $\hat{t}_c = t_c$ . As the  $SNR$  decreases, the estimate  $\hat{t}_c$  should vary around the right  $t_c$  but, in average,  $\hat{t}_c$  should equal the real  $t_c$ . It has been observed [3] that this sub-optimal estimator of  $t_c$  provides accurate enough values, at least in the range  $t_c \in [-\frac{T}{2}, \frac{T}{2}]$ , where the detection issue is most critical. Furthermore, the *phase-based estimator* (9) does not need the knowledge of  $t_c$  to determine the signal frequency and *remains statistically efficient over a large range of values for  $t_c$* . Hence, we keep this simple and fast technique in the sequel.

- [3] also shows that the ML estimator applied to noise only would produce aberrant values for  $\hat{f}_d$ , whereas the phase-based estimator does not.

To summarize, we propose the following scheme for solving the on-line detection/estimation problem:

#### Joint detection/estimation procedure

1. Acquisition of a new set  $\mathbf{x}$  of  $N$  samples, or of the last sample appeared for on-line application, from the anemometer.
2. Estimation of the parameter vector  $\hat{\theta}$ .  $\hat{f}_d$  will be the estimated frequency as in (9) in a recursive way;  $\hat{t}_c$  the parameter given by the sub-optimal method (11). Once  $(f_d, t_c)$  has been determined,  $\hat{s}_c$  is computed with (1) and ML estimates provide  $\hat{A} = \frac{\hat{s}_c^H \mathbf{x}}{\hat{s}_c^H \hat{s}_c}$  and  $\hat{\sigma}_b^2 = \frac{\|\mathbf{x} - \hat{A} \hat{s}_c\|^2}{2T+1}$  [1].
3. Computation of the log-likelihood ratio test  $\hat{l}(\mathbf{x})$  (3) using estimated parameters. Then comparison of  $\hat{l}(\mathbf{x})$  with the chosen threshold  $\gamma$  to decide under which hypothesis is this signal  $\mathbf{x}$ . Under  $\mathbf{H}_0$ , we do not give any sense to the vector  $\hat{\theta}$  found and go back to 1.
4. When  $\mathbf{H}_1$  is declared to be true, because of the sub-optimal estimator (11) of  $t_c$  used and because of the behavior of the CRB on  $f_d$  (see [1]), if  $\hat{t}_c \notin [-10, 10]$ ,  $\hat{\theta}$  is not considered as valuable enough

so we go back to step 1 again. In the other case, the actual value of  $\hat{\theta}$  is considered as valid.

#### 4. NUMERICAL EXAMPLES.

In this section, we present some numerical examples in order to illustrate the performances of the on-line estimation/detection scheme built here. Its performances will be characterized by the statistics of the estimated frequencies and the calculated  $P_{FA}$ ,  $P_D$  as described now:

- The probability of false alarm is estimated by:

$$\hat{P}_{FA} = \frac{\hat{I}(\mathbf{x}) \geq \gamma \text{ whereas } t_c \notin [-2T; 2T]}{\text{total number of cases}} \quad (12)$$

- We will distinguish two kind of probability of detection. The first one is given by:

$$\hat{P}_D^{[\pm 2T]} = \frac{\hat{I}(\mathbf{x}) \geq \gamma \text{ when } t_c \in [-2T; 2T]}{\text{total number of cases}} \quad (13)$$

This corresponds to the actual  $P_D$ , as defined in (5). However, what is of utmost importance is not to miss any particle whenever  $t_c \in [-\frac{T}{2}, \frac{T}{2}]$ . Hence, if  $H_0$  is assumed true -whereas  $H_1$  holds- when  $t_c \notin [-\frac{T}{2}, \frac{T}{2}]$ , this cannot be considered as a non-detection. Therefore, we define the following “modified” probability of detection as:

$$\hat{P}_D^{[\pm \frac{T}{2}]} = \frac{\hat{I}(\mathbf{x}) \geq \gamma \text{ when } t_c \in [-\frac{T}{2}, \frac{T}{2}]}{\text{total number of cases}} \quad (14)$$

##### 4.1. Simulated data.

First, we estimate the performances of the method by means of Monte-Carlo simulations where 500 trials were run. In these simulations, we generate  $x(t)$  according to (1) with  $b(t)$  circularly white Gaussian noise,  $T = 125$ ;  $M = 40$ ;  $f_d = 0, 02$  (case #1);  $0, 05$  (#2) and  $0, 10$  (#3);  $\alpha = 0, 1228$ ;  $SNR = 10\text{dB}$ ;  $A = e^{j\varphi}$  (where  $\varphi$  is uniformly distributed on  $[0, 2\pi]$ ) and  $t_c \in [-3T, 3T]$ . Hence, from the definition of the two hypotheses, for  $t_c \in [-3T, -2T] \cup [2T, 3T]$  the signal is under  $H_0$  whereas for  $t_c \in [-2T, 2T]$   $H_1$  holds. Table 1 gives the numerical values of empirical probabilities. Figure 2 reports the results of this simulation for  $f_d = 0, 10$  only. The mean of  $\hat{f}_d$ , the square-root of its variance and the square-root of the corresponding theoretical CRB (derived in [1]) -when they are considered as valid- are given in Table 2. As can be seen, the on-line detection scheme proposed here provides good detection probabilities, at least when  $t_c \in [-\frac{T}{2}, \frac{T}{2}]$ .

As expected,  $\hat{P}_D^{[\pm 2T]}$  is inferior to  $\hat{P}_D^{[\pm \frac{T}{2}]}$  which reaches 100%. Additionally, the probability of false alarm remains very low, mainly because  $\gamma > 0$ . When the estimation is considered as valid the signal's parameters found are very close to the simulation ones, since they exhibit a variance close to the CRB (see Table 2).

##### 4.2. Real data.

We present now results which emphasize the effectiveness of this detection/estimation scheme when applied to **real data**. The laser anemometer considered has been tested during an on-board flight trial. 2998272 data samples were delivered during this flight. The

developed method was applied to a sliding window of length  $N = 701$  samples ( $T = 350$ ), shifted one sample at a time. The number of correlation lags was taken equal to  $M = 115$ . As in the numerical simulations, **only** when  $H_1$  is assumed to be true and  $|\hat{f}_c| \leq 10$ , the test is positive.  $\hat{f}_d$  is then stored and compared with the exact Doppler frequency provided by the speed of flight measured by a Pitot tube. We know that **2928** particles crossed the probe volume during this flight test and generated **useful laser signals** (named *Bursts*) corresponding to various speeds of the flight (between  $30 \text{ m.s}^{-1}$  during take off and  $270 \text{ m.s}^{-1}$  during cruise flight). Moreover, the appearance instant of each of these *bursts* was recorded. With these two a-priori informations, when the test is positive, we can conclude if it really corresponds to a *burst* or if it is a false alarm. So, we are able to calculate the corresponding  $P_{FA}$  and/or  $P_D$ . Over all the treated samples, the on-line LRT test declared 2918 signals. Each of these detection's cases corresponded to appearance instant of recorded *bursts*. So, in this real application, **2918 out of 2928 particles** crossing the probe volume **were detected**. Moreover, for each of these cases, the second condition  $-10 \leq \hat{f}_c \leq 10$  **was fulfilled -in average- for more than 20 successive recorded samples**. Hence, for this real application, the Probability of Detection equals  $\hat{P}_D = \frac{2918}{2928} = 99,66\%$ . This first result of the detection scheme is in accordance with the above theory since  $\gamma$  was determined such that  $P_D \geq 99,5\%$ . When the two validating conditions appeared on several successive samples for a same *burst*, we calculated the corresponding signal frequency by taking the mean of all the frequencies estimated by (9). Figure 3 reports this result and compares estimated frequencies with the measured ones. When *bursts* were acquired, the estimated speed and the exact one are in very good agreement since the two corresponding plots are superimposed. Hence, **10** of the recorded signals have **not been detected** mainly because of a too low SNR level. Finally, there is **no detection's cases of the LRT (3)** which do **not correspond** to the passage of an aerosol. So, we have to conclude to a Probability of False Alarm of  $\hat{P}_{FA} = 0\%$ : theoretically  $\gamma > 0$  shall ensure  $P_{FA} = 0$ . Table 3 summarizes the results obtained. Hence, this real application confirms the numerical simulations and their results.

#### 5. CONCLUSION.

In this paper, we considered the problem of estimating aircrafts' speed from on-board laser anemometer. Since the flow is not continuous, aerosol particles cross the probe volume in a random way. So, we addressed the problem of simultaneously detecting the presence of aerosol and estimating its speed. A Likelihood Ratio Test was presented and solutions for choosing the threshold were proposed. Computationally efficient on-line estimators of the parameters of interest were derived. The joint detection/estimation scheme was successfully applied to real data recorded on-board an aircraft. It corroborated the results obtained on simulated data.

#### 6. REFERENCES

- [1] O. Besson and F. Galtier. Estimating particle's velocity from laser measurements: Maximum Likelihood and Cramér-Rao bounds. *IEEE Transactions Signal Processing*, 44(12), December 1996.

- [2] F. Galtier and O. Besson. Frequency estimation of laser signals with time-varying amplitude from phase measurements. *Proceedings ICASSP*, pp. 4005-4008, April 1997, Munich.
- [3] F. Galtier and O. Besson. On-line Joint Detection of Particle's Arrival and Estimation of Speed in Laser Anemometry. *submitted to Signal Processing*.
- [4] L.L. Scharf. *Statistical Signal Processing: Detection, Estimation and Time Series Analysis*. Addison Wesley, Reading, MA, 1991.
- [5] H.L. Van Trees. *Detection, Estimation and Modulation Theory*. John Wiley, New York, 1971

Estimated	$\hat{P}_{FA}$	$\hat{P}_D^{[\pm 2T]}$	$\hat{P}_D^{[\pm \frac{T}{2}]}$
Case #1	0,29%	72,56%	100%
Case #2	0,33%	70,95%	100%
Case #3	0,45%	68,83%	100%

Table 1: Estimated values of  $P_{FA}$ ,  $P_D^{[\pm 2T]}$  and  $P_D^{[\pm \frac{T}{2}]}$  from the detection/estimation scheme proposed.

Mean values	$f_d$	$\sqrt{CRB}(f_d)$
theoretical #1	0,02	$1,301.10^{-5}$
estimated #1	0,0200	$\pm 1,338.10^{-5}$
theoretical #2	0,05	$1,145.10^{-5}$
estimated #2	0,0500	$\pm 5,148.10^{-5}$
theoretical #3	0,10	$1,455.10^{-4}$
estimated #3	0,1000	$\pm 1,525.10^{-4}$

Table 2: Mean values of the parameters estimated from the detection/estimation scheme proposed.

Number of samples	Detected bursts	$P_D$	False Alarms	$P_{FA}$
2998272	2918	99,66%	0	0%

Table 3:  $\hat{P}_{FA}$ ,  $\hat{P}_D$  of the detection/estimation scheme proposed applied to real flight data.

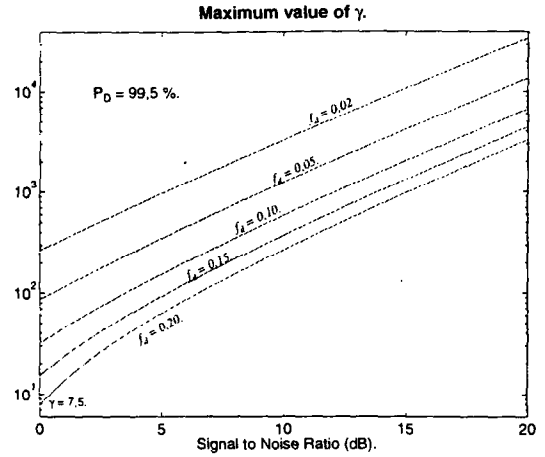


Figure 1: Maximum  $\gamma$  ensuring  $P_D > 0,995$  for  $t_c = -\frac{T}{2}$ , versus  $SNR$  and  $f_d$ .

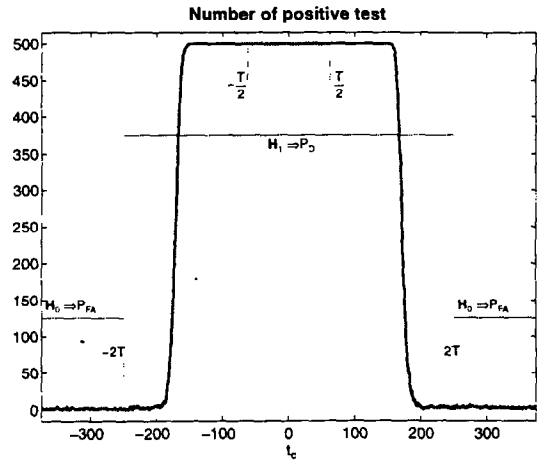


Figure 2:  $\hat{P}_{FA}$ ,  $\hat{P}_D$  versus  $t_c$ .  $f_d = 0, 10$  and  $SNR = 10$  dB.

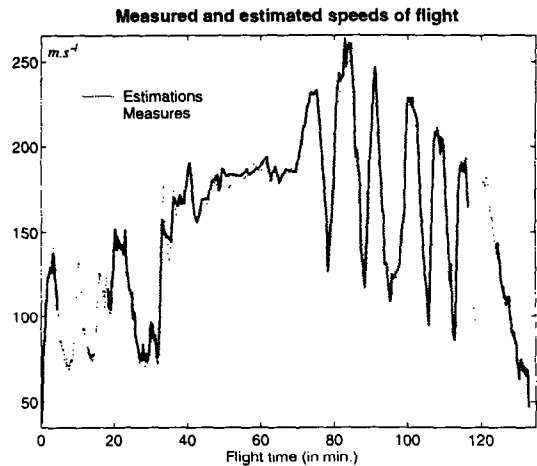


Figure 3: Estimated and measured speed during the flight trial of the laser anemometer.